Chapter 7

Possible Applications of Fluoro Protein Chromophore Coupled Photomagnetic Diradicals

The design, characterisation and application of three different pairs of imino nitroxide based green fluorescent protein chromophore and its different homologue coupled diradicals have been theoretically studied in this chapter. To begin with, the geometries of all these diradicals have been optimized at high spin state in gas phase, in water medium and in blood plasma medium. For calculations in water medium, we have adopted the 2-layer our own N-layer integrated molecular orbital and molecular mechanics (ONIOM) method. Similarly for blood phase calculations, the polarized continuum model (PCM) method has been adopted. With these optimized geometries the magnetic exchange coupling constant (J) values are estimated for these diradicals in different medium using broken symmetry (BS) approach in unrestricted DFT framework. We have found that these diradicals have an ability to change their magnetic nature from antiferromagnetic in trans form to ferromagnetic in cis form upon irradiation with light of appropriate wavelength. Using time dependent DFT (TDDFT) technique the required wavelengths of light by which non-fluorescent dark trans diradicals turn into their corresponding bright fluorescent cis isomers, are determined for each pair of diradicals for gas and water medium. This color change which can be observed in bare eyes is indeed a signature of the change in magnetic state of the diradicals concerned. Moreover, we have also calculated the zero field splitting (ZFS) parameter (D), rhombic ZFS parameter (E) and ZFS magnitude (a_2). From our calculations we ambitiously expect that if these diradicals are synthesized then they can be used as successful, non-hazardous magnetic resonance imaging contrast agent (MRICA) in place of other metal based contrast agents.

7.1. Introduction

Materials science research has gained notable importance in the field of biomedical research through design, preparation and appliance of effective multifunctional biomaterials.[1-3] Some of these multifunctional systems are useful because they exhibit magnetic behavior in reduced dimension. The fundamental requirement for developing multifunctional nano-magnetic material is to design ferromagnetic molecules with diverse functional characteristics such as photosensitivity, fluorescence activity, water solubility etc. These types of multifunctional molecules have earned huge interest in the lurking field of materials science research.[4] Following this trend, attention has been given on designing photomagnetic molecules which change their magnetic behavior when exposed to suitable external radiation.[5] Thus, these systems can be activated or deactivated by appropriate irradiation as required for effective use of their magnetic property. Nevertheless, magnetic field induced magnetization reversal procedure for magnetically active molecules is well known and used for diverse technological applications.[6] However, this process is difficult to implement as it requires very high field gradient. On the other hand, compared to the field induced process, photoinduced magnetic crossover is easier to accomplish and more suitable for functional uses.[7]

Photochromic molecules undergo photon induced reversible chemical change involving two different wavelengths of electromagnetic radiation and instantaneously modulate their geometries and physical properties. If two monoradical moieties are connected with such photochromic coupler of particular structural form the resulting diradical switch to another structural form of the coupler by a definite external electromagnetic radiation.[8] As a result, change in magnetic property due to this structural change is observed. The photomagnetic behavior of substituted pyrene molecules has been nicely studied by Ali and Datta.[9] Photoinduced antiferromagnetic to ferromagnetic crossover in case of organic diradicals has also been reported and widely studied very recently.[5]

Fluorescent proteins, with photochromic property have revolutionized the study of living cells. The first such protein utilized in cell biology was green fluorescent protein

(GFP) which was obtained from jellyfish *Aequorea Victoria.*[10] The GFP has found its use in cellular and molecular biology, genetics, medicines and chemistry over the past several years.[10,11] This has also initiated several studies on different natural and artificial homologues of GFP.[12,13] The structural aspects and uses of GFP and its various homologues are nicely illustrated in the detailed review of Zimmer.[13]

Photomagnetic molecules with GFP chromophore and its homologues based diradicals have recently been designed and studied by Bhattacharya et al.[5(b)] There is certainly a possibility of developing multifunctional photochromic ferromagnetic molecules with GFP and its different derivatives as couplers which are expected to show fluorescence properties in addition to the ferromagnetic properties. Existence of both magnetic and fluorescence properties in same molecule will certainly make them a potent candidate for different biomedical applications particularly in the field of magnetic resonance imaging (MRI). The site specific MRI contrast agent (MRICA) with increased rate of relaxation of water protons in the targeted tissues, makes MRI fascinating in the field of *in vivo* bimolecular imaging. Most widely used MRICAs are various Gd-chelate compounds. However, Gd ion being poisonous in nature, toxic effect of Gd ion due to accidental *in vivo* dissociation of the Gd-chelate can not be avoided causing renal failure of patient after MRI investigation.[14] An alternative way is to use radical based organic MRICAs like nitroxide-leveled anti-cancer drug lomustine.[15] The point to be noted here is that a successful MRICA should be anti toxic, water soluble, biocompatible, easily renal excreable, and most importantly *in vivo* stable. Moreover, it should have greater volume distribution and better cell permeability. So far, among the synthesized stable radicals, nitroxyl radicals possess these qualities making themselves suitable for designing of MRICA.[16] Moreover, pyrrolidine and piperidine type nitroxyl radicals have the ability to cross the blood brain barrier (BBB) which is the primary requirement for a MRICA to be suitable for brain MRI scan.[15]

In this chapter, we have used (1) *p*-HBDI, (2) *m*-HBDI and (3) BFPF as fluorescent couplers with imino nitroxide (IN) as magnetic center to construct the diradicals. In every case trans-isomers of diradicals are designated as (a) and its corresponding cis-isomers are indicated as (b). Diradicals attached to the trans and cis states of GFP type coupler absorb

Scheme 7.1. Pictographic representation of reversible trans-cis photoisomerization of green fluorescent protein chromophore based diradicals (1-3). Where, X is imino nitroxide (IN) moiety and Y represents the fragment of the particular chromophore. Here, τ and φ stands for the dihedral angles as shown.

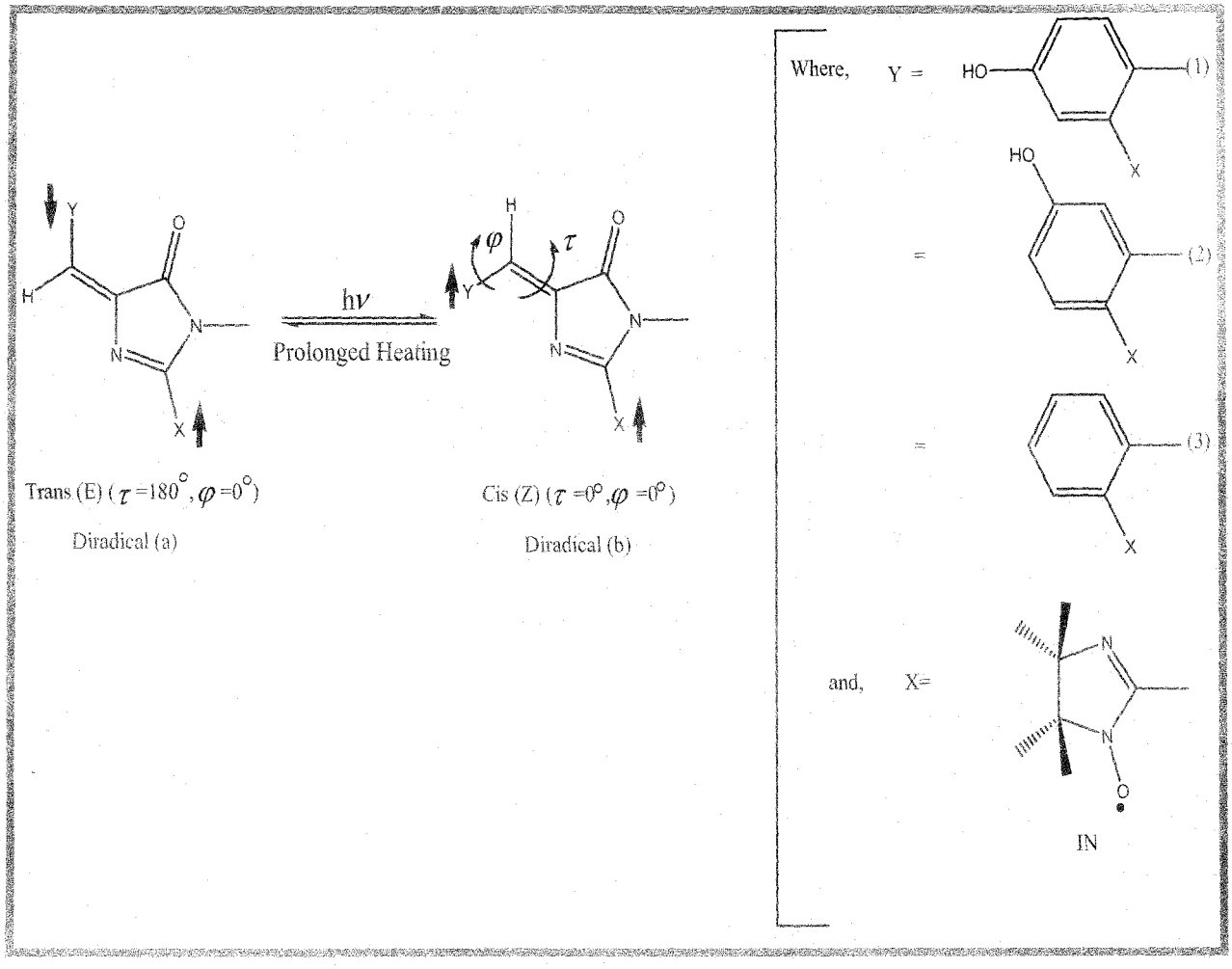

two different wavelengths and interchange their states as well as the nature of magnetism depending upon the state of GFP coupler to which it is attached. We choose the imino nitroxide radical because of its stability, non-toxicity and solubility in water medium.[17] These designed diradicals are useful in making water soluble photoswitchable magnetic molecules with fluorescence properties observable in naked eye. The whole process is shown in Scheme 7.1. We have estimated the magnetic exchange coupling constant values (J) for two different forms of every diradical in gas phase. We have also evaluated their J values in water and

blood plasma medium to understand their *in vivo* suitability. By writing *blood plasma* in italics we really mean that we have taken an average condition of a very complicated physiological fluid, blood. Throughout this article the same has been referred as "blood" in several occasions. The relative stability of the designed diradicals in different medium with respect to the total energy value is discussed. In every medium we have observed a magnetic crossover from antiferro- to ferro-magnetic states when the trans forms of each diradical is exposed to suitable wavelength of light. The required wavelength of external radiation is estimated through time dependent density functional theory (TDDFT) based calculations both in gas phase and in water medium. To know the suitability of our designed diradicals as MRICAs, we have evaluated their zero field splitting (ZFS) parameters and compared with other synthesized molecular systems which are already in use as MRICAs.

7.2. Theoretical Background and Methodology

The exchange interaction between two magnetic sites 1 and 2, is in general expressed by the Heisenberg spin Hamiltonian, $\hat{H} = -2J\hat{S}_1 \cdot \hat{S}_2$, where $\hat{S}_1$ and $\hat{S}_2$ are the spin angular momentum operators of site 1 and 2 respectively and J is the exchange coupling constant. A positive J value indicates ferromagnetic interaction whereas the negative value of J signifies antiferromagnetic interaction. To evaluate the exchange coupling constant with reasonably less computational effort, Noodleman[18] has proposed an unrestricted spin polarized broken symmetry (BS) formalism in DFT framework. The BS state is not a pure spin state but a state of mixed spin symmetry with lower spatial symmetry. Depending on the extent of magnetic interaction between two magnetic sites, many scientists have developed different formulae to estimate J using the BS approach.[18-20] Ideally, for diradicals the computed average $<S^2>$ values for triplet and BS states should be exactly 2.00 or 1.00 respectively. However in reality, their difference is not exactly unity showing a clear indication of spin contamination problem. In order to neutralize the spin contamination error associated with the BS state, one can use spin projection technique. For estimating the J values of diradicals of organic origin, the following expression by Yamaguchi et al.[19] is the most widely applied[5,9,21] and has been used by us in this chapter. This expression is given by

$$J = \frac{(E_{BS} - E_{HS})}{\langle S^2 \rangle_{HS} - \langle S^2 \rangle_{BS}}, \tag{7.1}$$

where E_{BS}, $\langle S^2 \rangle_{BS}$ and E_{HS}, $\langle S^2 \rangle_{HS}$ are the energy and average spin square values for corresponding BS and high spin states respectively.

As far as the biomedical applications are concerned, gas phase calculations of molecular energies are unlikely to produce a reliable picture. A more realistic approach is to consider the molecule-medium interaction. To achieve this end, one can employ the Our own N-layer Integrated molecular Orbital molecular Mechanics (ONIOM) method. In this method the whole system is divided into several onion-like layers. Out of which the inner active centre is treated with highest level *ab initio* QM method while the outer layer is treated with low-level QM or MM method. In a two layer hybrid ONIOM (high: low) method the extrapolated energy of the real system at high level is given by

$$E_{total}^{ONIOM} = E_{core}^{high} + E_{total}^{low} - E_{core}^{low}, \tag{7.2}$$

where 'high' and 'low' refers to high- and low-level theoretical methods. The subscripts 'core' and 'total' indicate the active site and the whole system respectively. Explicit solvation effect on the triplet geometry and triplet energy can be obtained from the ONIOM optimized geometry of the diradical molecule. A similar calculation using BS state of the inner high level layer will give the solvation effect on the energy of BS state. The method is named as ONIOM-BS method.[22]

Another way of considering the effect of medium on molecule is to apply polarized continuum model (PCM) method. This method, proposed by Newton,[23] evaluates the solute charge density distribution in dielectric continuum by solving the Schrödinger equation self consistently. The method considers that a molecule has a definite shape and effective volume and it is rarely spherical. Moreover, half the diameter of the solvent molecule is added with the constructed boundary of the solute molecule. In most cases the solvent is water unless specified and in general 0.5Å is added leading to slight error. As this method relies on self

consistency, it is valid for any order and one can perform PCM calculations for various quantum chemical methods like DFT, perturbation theory etc. Using PCM one can also optimize molecular geometry. The PCM method actually considers medium as a dielectric continuum and any averaging is included in the dielectric constant. As a matter of fact, PCM does not explicitly consider any fluctuation effect from average solvent polarization.[24] For all three diradical pairs PCM optimization calculations have been carried out taking *blood plasma* (ε = 58) as medium. With the PCM optimized geometry of these diradicals in high spin state, the BS treatment has been performed to know the magnetic nature of these molecules in *blood plasma* medium. This method is named as PCM-BS method.

It is known that the spectroscopic and photochemical properties of any photoactive molecule can be well comprehended by knowing the ground and excited state energies of the molecule. For any photoinduced chemical process involving chromophore, it is necessary to know the transition energy barrier between the two photo reactive forms of the species. It has been observed that the transition energy barrier has close correspondence with the excitation energy of the chromophoric molecule. To be more specific, in the different variants of GFP chromophores the excitation would take place from bonding (π) to antibonding (π^*) orbitals. It is already known that, the post Hartree Fock methods are suitable to estimate the wave length of external radiation for electronic transition in molecular systems.[25] However, they are also computationally expensive and following our recent works,[5(a),5(b)] we have employed time dependent density functional theory (TDDFT)[26] based calculations, which is a way out to obtain electronic excitation energies with less computational efforts.[27] The TDDFT method, relies on the frequency dependent polarizability of a system, and produces more reliable results than other methods.[28] On the other hand, TDDFT is almost free from "near triplet instability"[29] error and in addition the excited state energies from filled to unfilled orbitals can be obtained by performing only ground state Kohn-Sham calculations.[30,31]

The TDDFT method is based on the dynamic polarizability $\overline{\alpha}(\omega)$ of a system which has poles at frequencies analogous to its transition energies. Obtaining the frequency dependent polarizability from TDDFT calculations and substituting it in the sum-over-states relation

$$\bar{\alpha}(\omega) = \sum_I \frac{f_I}{\omega_I^2 - \omega^2}, \tag{7.3}$$

one can get oscillator strength (f_I) and excitation frequency (ω_I) respectively.[29] We calculate $\pi \rightarrow \pi^*$ transition energies for all designed trans fluorescent protein chromophores following the above method. All these above mentioned computations are implemented through Gaussian 09W quantum chemical package.[32]

Rajca and coworkers have established that the diradical and polyradical systems with organic origin can be successfully used as MRI contrast agent.[33] For the rational designing of MRICA one needs to know the extent of zero field splitting (ZFS) in addition to the solubility criterion. The ZFS, associated with magnetic anisotropy, is one of the important parameters to investigate the geometric and electronic properties of a radical with $S > ½$.[34] Having known the ZFS, one can easily estimate the electron spin correlation time which is one of the governing factors for clearer MRI scans with enhanced contrast.[35]

The ZFS arises from two contributions, namely the direct electron-electron magnetic dipole spin-spin (SS) interaction and the spin-orbit coupling (SOC) of the electronically excited state with the ground state.[34] It has also been established from the earlier work that the SS coupling happens to be the main source of ZFS in case of organic diradicals.[36] The ZFS value arising from the SS interactions can be estimated through effective spin Hamiltonian

$$\hat{H}_{ZFS} = \sum_{ij} \boldsymbol{D}_{ij} \hat{S}_i \hat{S}_j, \tag{7.4}$$

where $\boldsymbol{D}_{ij}$ is the ZFS tensor, $\hat{S}_k$ is the k'th Cartesian component of the total electron spin operator. For a diagonalized $\boldsymbol{D}_{ij}$ one can write the Hamiltonian as

$$\hat{H}_{ZFS} = D\left(\hat{S}_z^2 - \frac{1}{3}\hat{S}^2\right) + E\left(\hat{S}_x^2 - \hat{S}_y^2\right), \tag{7.5}$$

where D and E are the axial and rhombic ZFS parameters respectively.[37]

The first order contribution to the ZFS energy using the single ground state Kohn-Sham determinant is the SS coupling part of the ZFS and it can be calculated by applying the following formula[38]

$$D_{kl}^{(SS)} = \frac{g_e}{4}\frac{\alpha^2}{S(2S-1)}\left\langle 0SM_S \left| \sum_i \sum_{j\neq i} \frac{r_{ij}^2\delta_{kl} - 3(r_{ij})_k(r_{ij})_l}{r_{ij}^5} \times \left\{ 2\hat{S}_{iz}\hat{S}_{jz} - \hat{S}_{ix}\hat{S}_{jx} - \hat{S}_{iy}\hat{S}_{jy} \right\} \right| 0SM_S \right\rangle, \tag{7.6}$$

where α is the fine structure constant, g_e is the gyromagnetic ratio. The operators $\hat{S}_{mn}$ signify n'th component of m'th spin vector and r_{ij} is the magnitude of the distance vector between spins i and j. The equation can be safely approximated as[39]

$$D_{kl}^{(SS)} = \frac{g_e}{4}\frac{\alpha^2}{S(2S-1)}\sum_{\mu\nu}\sum_{\kappa\lambda}\left\{ P_{\mu\nu}^{\alpha-\beta}P_{\kappa\lambda}^{\alpha-\beta} - P_{\mu\kappa}^{\alpha-\beta}P_{\nu\lambda}^{\alpha-\beta} \right\} \times \left\langle \mu\nu \left| r_{12}^{-5} \left\{ \left\{ 3r_{12,k}r_{12,l} \right\} - \delta_{kl}r_{12}^2 \right\} \right| \kappa\lambda \right\rangle, \tag{7.7}$$

where $P^{\alpha-\beta} = P^{\alpha} - P^{\beta}$ the spin density matrix in the atomic orbital basis, and μ, ν, κ and λ are the basis functions.[36] These tensor elements can be used to evaluate the ZFS parameters D and E.[40] The D and E values are utilized to determine the static ZFS magnitude (a_2) using the formula

$$a_2 = \sqrt{\left(\frac{2}{3}D^2 + 2E^2 \right)}. \tag{7.8}$$

From this a_2 longitudinal electron spin relaxation rate $\frac{1}{T_{1e}}$ can be estimated following the expression[41]

$$\frac{1}{T_{1e}(B_0)} = \frac{2}{5}a_2^2\tau_R\left[\frac{1}{1+\omega_0^2\tau_2^2} + \frac{4}{1+4\omega_0^2\tau_2^2} \right] + \frac{12}{5}a_{2T}^2\tau'\left[\frac{1}{1+\omega_0^2\tau'^2} + \frac{4}{1+4\omega_0^2\tau'^2} \right], \tag{7.9}$$

where B_0 is the external magnetic field, ω_0 is the Larmor frequency, τ_2 and τ' are the reduced spectral densities and a_{2T} is the transient ZFS magnitude.[42] Larger a_2 corresponds to

a faster relaxation rate $\frac{1}{T_{1e}}$.[41] Here B3LYP correlation functional along with 6-31G(d,p) basis set has been used in the unrestricted formalism for the calculation of D and a_2.

7.3. Results and Discussion

The gas phase molecular geometries of all three cis-trans pairs have been fully optimized with the unrestricted B3LYP exchange correlation functional using 6-31G(d,p)

Table 7.1. The gas phase single molecule optimized energies (in *au*) for trans and their corresponding cis forms of all 3 sets of diradicals. The $\langle S^2 \rangle$ values and corresponding exchange coupling constants (J in cm^{-1}) are also reported. The calculations are done using UB3LYP level of theory with 6-311++G(d,p) basis set.

Diradical		At UB3LYP/6-311++G(d,p) level		
		Energy(*au*)	$\langle S^2 \rangle$	$J(cm^{-1})$
1a	Triplet	– 1601.62893	2.037	–8.8
	BS	– 1601.62897	1.038	
1b	Triplet	– 1601.63404	2.038	2.2
	BS	– 1601.63403	1.036	
2a	Triplet	– 1601.62905	2.035	–8.8
	BS	– 1601.62909	1.040	
2b	Triplet	– 1601.63386	2.037	8.8
	BS	– 1601.63382	1.034	
3a	Triplet	–1526.38116	2.036	–8.8
	BS	–1526.38120	1.038	
3b	Triplet	–1526.38590	2.037	7.4
	BS	–1526.38589	1.741	

Scheme 7.2. Schematic representation of geometrical and exchange pattern of different photoconvertable GFP based antiferromagnetic (itinerant exchange) dark trans (1a, 2a and 3a) and their corresponding ferromagnetic (direct exchange) fluorescent cis (1b, 2b and 3b) diradicals taking imino nitroxide (IN) as radical centers. The red colored up and down arrows represent α and β spin respectively.

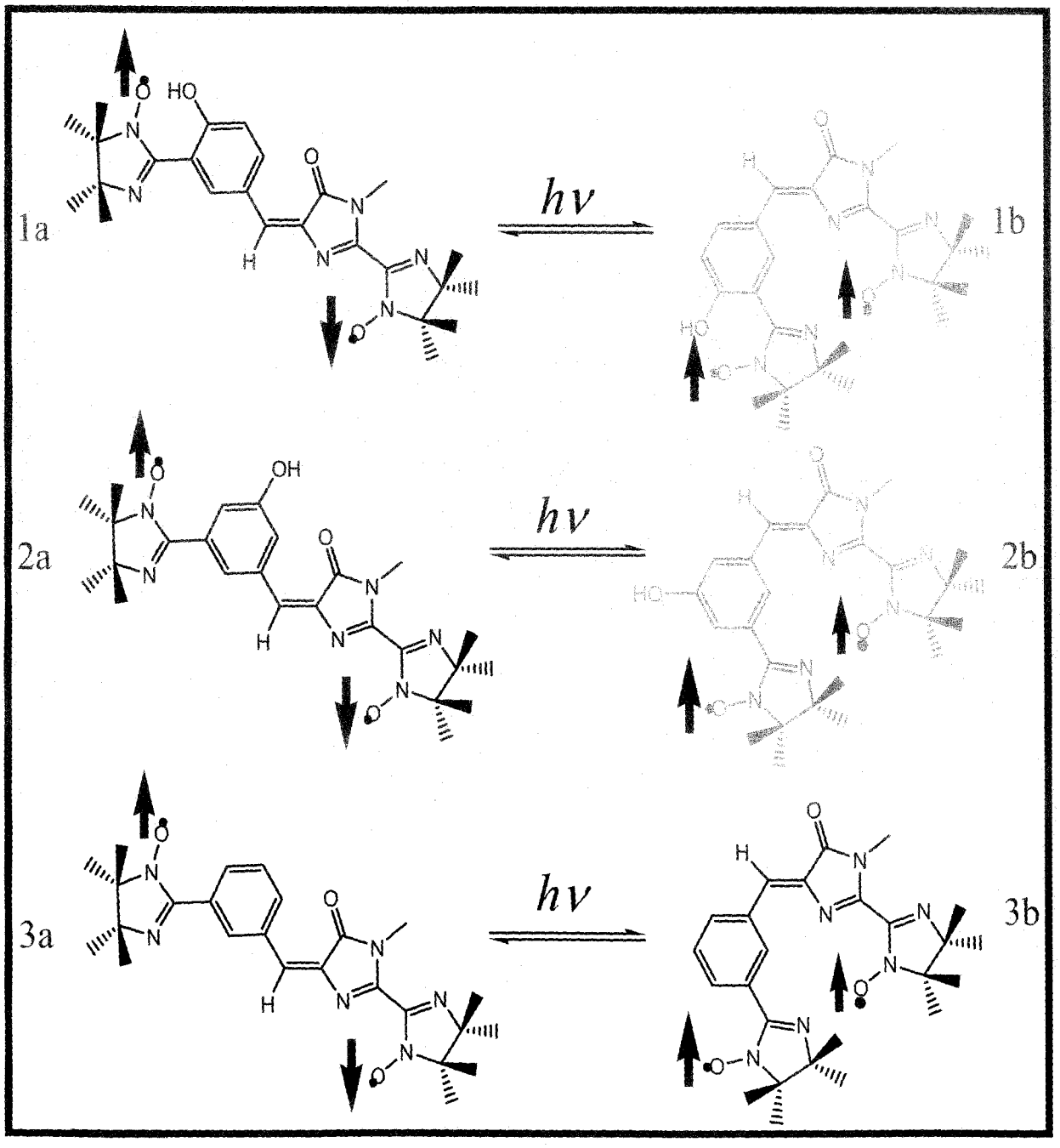

basis set. Scheme 7.2 shows the actual structure, exchange pattern and colors of all the ferromagnetic cis form and their corresponding dark antiferromagnetic trans form. The Figure 7.1 shows the gas phase optimized geometries. Based on these molecular geometries, the corresponding *J* values for each pair have been estimated from single point energies of the triplet and BS states at UB3LYP/6-311++G(d,p) level (eq 7.1). All the gas phase *J* values are shown in Table 7.1. Hence, antiferro- to ferro-magnetic crossover in all chosen diradical systems are observed when the trans isomers are exposed with proper electromagnetic radiation. It is also to be noted that, this type of magnetic crossover is associated with fluorescence color change, which can be viewed in naked eye. It is clear from Figure 7.1 that the trans form of all the diradicals are planar. They possess singlet ground state with opposite spin orientation in two different spin sites. In these isomers spin polarization is blocked through the coupler resulting in a manifestation of antiferromagnetic behavior. However, in the corresponding cis states of the respective diradicals the monoradical centers are out of plane in a manner that their close proximity facilitates direct exchange which results in ferromagnetism. The spin density plots admit the fact that although the spin density is less pronounced through the coupler, the direct exchange makes them magnetically active.[5(a-b)] The spin density distribution in gas phase optimization and in PCM optimization are depicted in Figure 7.2 and Figure 7.3 respectively.

To account for the solvent effect in the designed diradicals, we have performed ONIOM optimization (Figure 7.4) for each pair at UB3LYP/6-31G(d,p):UFF level treating the diradical as higher level and water as lower level in two level ONIOM. We take approximately 65 to 75 water molecules in low layer of ONIOM. The optimized geometries have been used for single point calculation of ONIOM-triplet and corresponding ONIOM-BS energies in UB3LYP/6-31G(d,p):UB3LYP/3-21G level of theory. The corresponding magnetic exchange coupling constant values obtained from the difference of ONIOM-triplet and ONIOM-BS energies using Yamaguchi formula are compiled in Table 7.2. Like that in gas phase here also we observe the antiferro- to ferro-magnetic crossover when explicit solvation model ONIOM method is considered. We have also taken into account the implicit solvation model using PCM technique. All the diradical pairs are optimized (Figure 7.5) at blood dielectric constant ($\varepsilon = 58$). We calculate the *J* values for all the diradicals through the

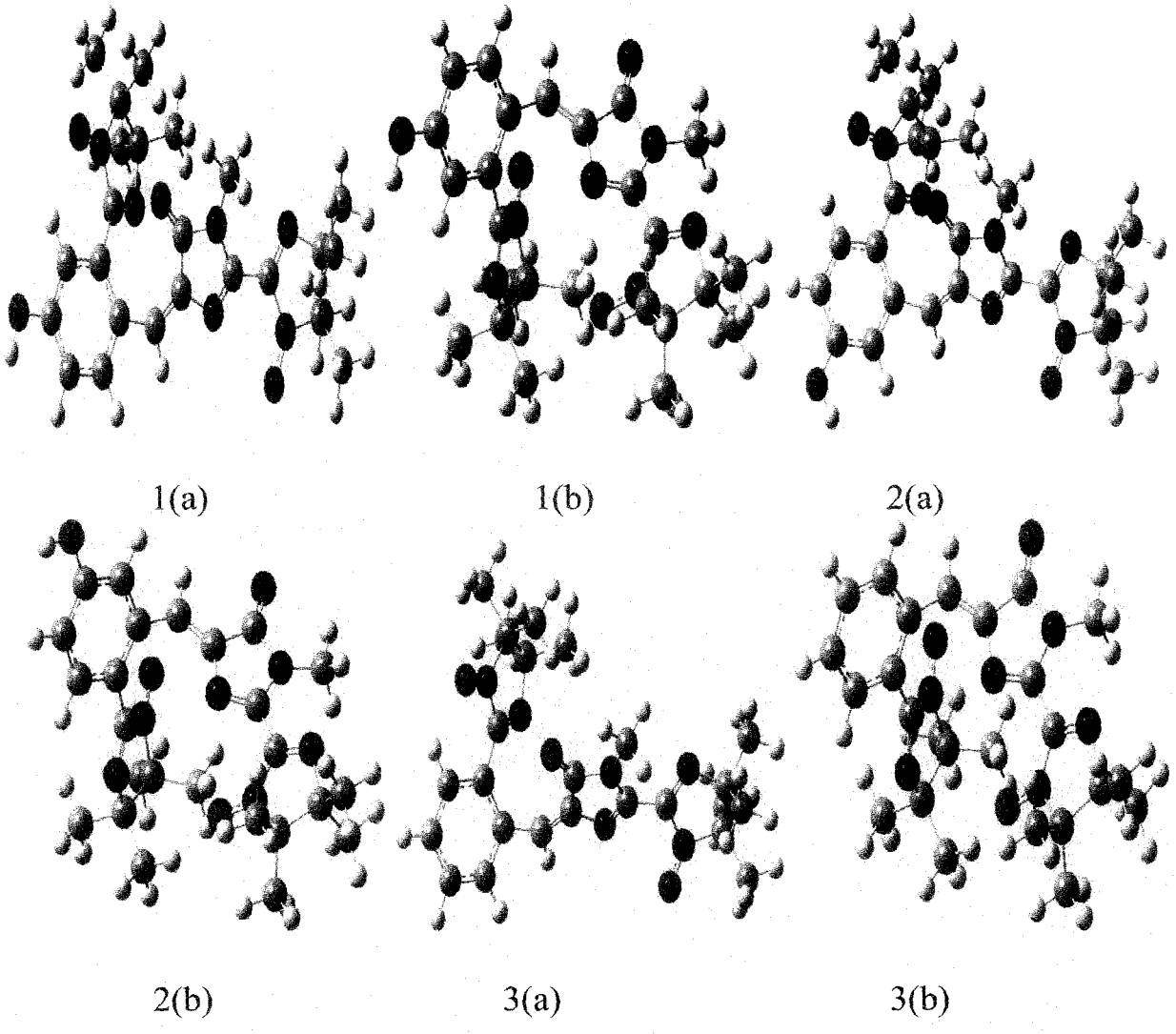

Figure 7.1. The gas phase optimized geometries of three trans (1a, 2a, 3a) diradicals and their corresponding cis forms (1b, 2b, 3b) with different GFP variants (*p*-HBDI, *m*-HBDI and BFPF respectively) as coupler. The geometries are optimized using UB3LYP method at 6-31G (d,p) level. The carbon atoms are represented in grey, nitrogen in blue, oxygen in red and hydrogen in white respectively.

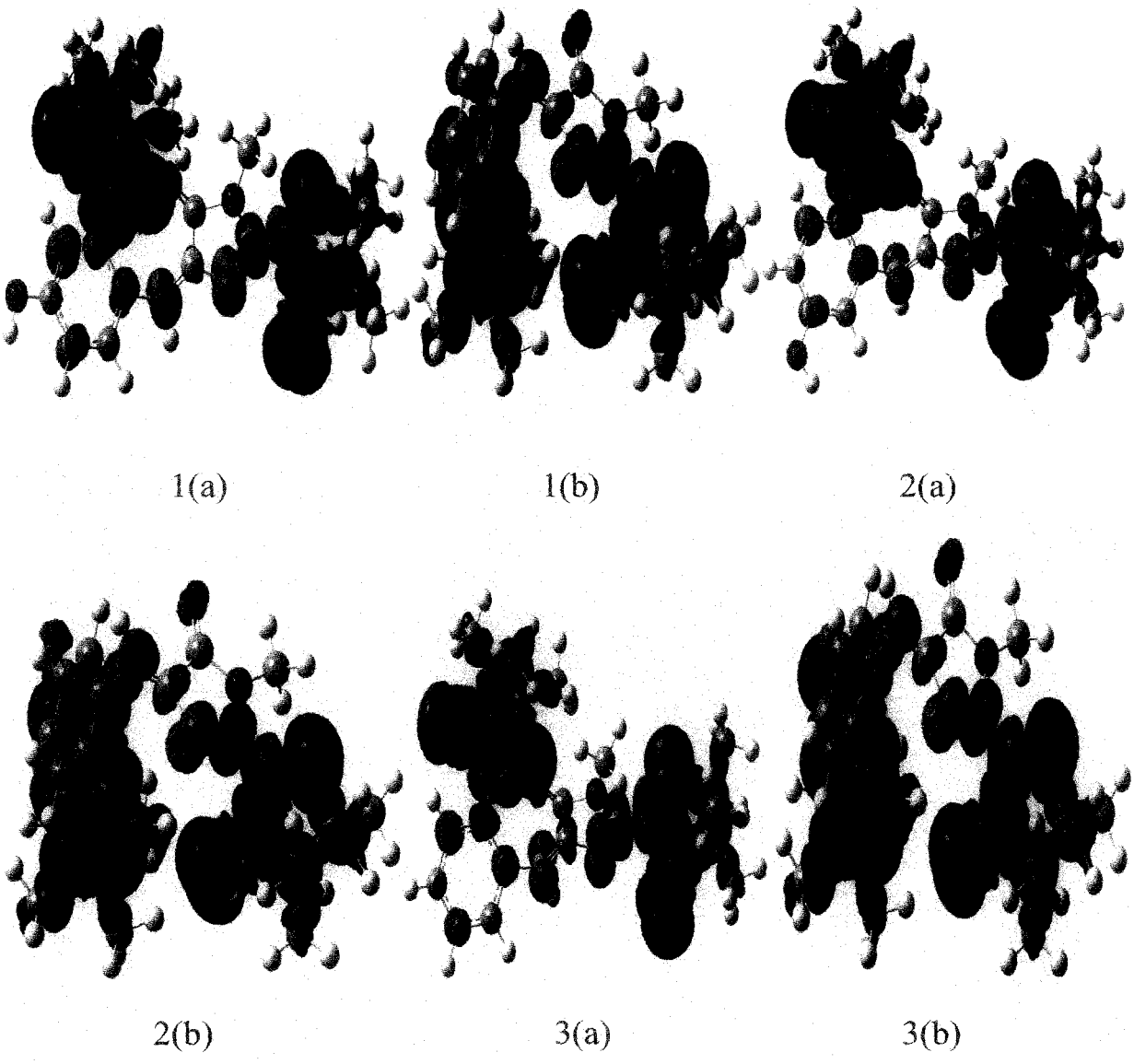

Figure 7.2. Gas phase spin-density plots for the diradicals in their triplet optimized states. Different color schemes are used for two different spins.

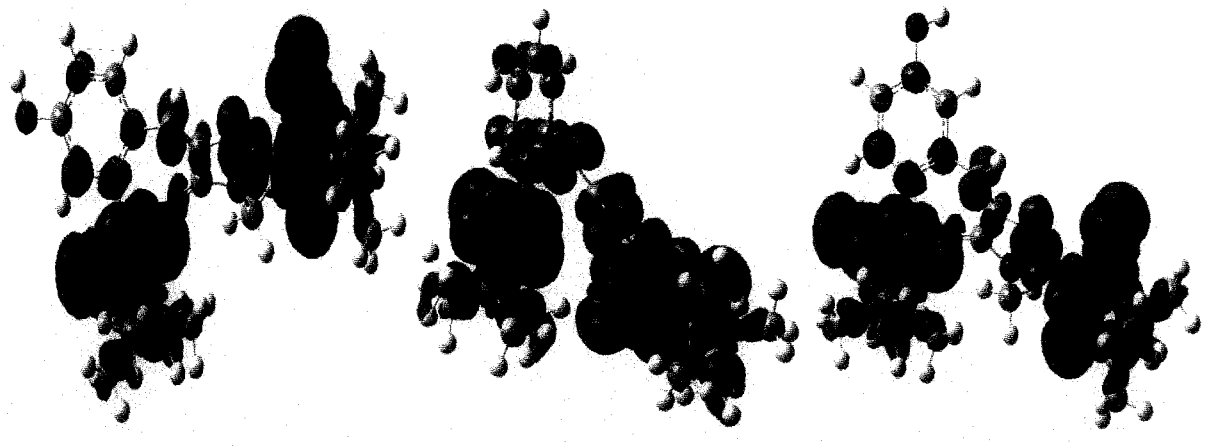

1(a) 1(b) 2(a)

2(b) 3(a) 3(b)

Figure 7.3. The spin-density plots for the triplet diradicals optimized using PCM method with $\varepsilon = 58$. Red and green color schemes are used for the representation of α and β spin respectively.

1(a) 1(b)

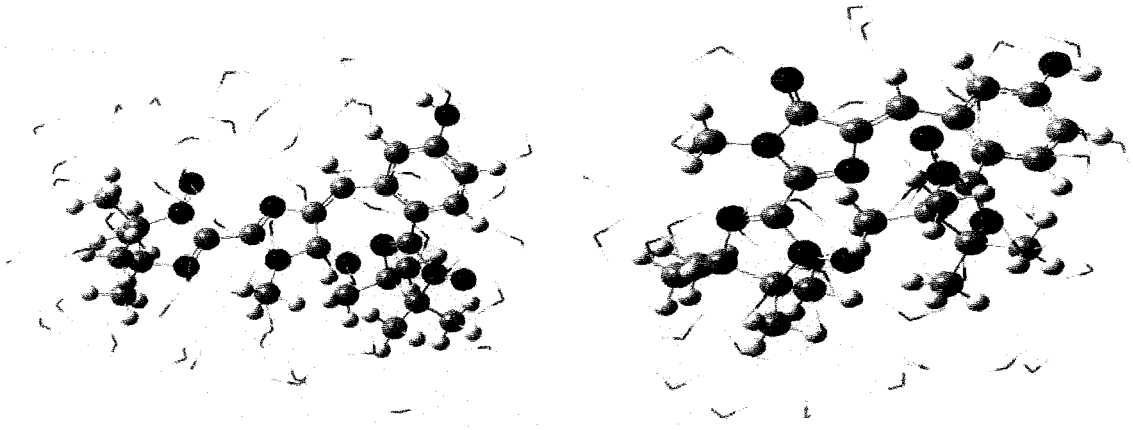

2(a) 2(b)

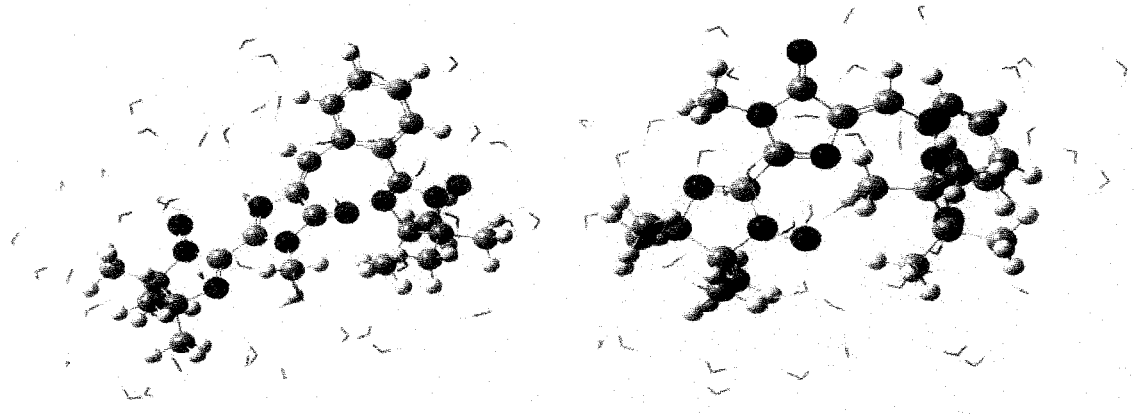

3(a) 3(b)

Figure 7.4. The ONIOM optimized geometries of water solvated 3 trans (1a, 2a, 3a) diradicals and their corresponding cis forms (1b, 2b, 3b) with different GFP variants (*p*-HBDI, *m*-HBDI and BFPF respectively) as coupler. The QM and MM levels are represented by ball and stick and only ball model respectively. The two layer ONIOM optimization for each diradical pairs are performed at UB3LYP/6-31G(d,p):UFF level; where the diradicals are treated as higher level (QM) and water molecules at lower level (MM). The carbon atoms are represented in grey, nitrogen in blue, oxygen in red and hydrogen in white respectively.

PCM-BS approach. The results of the PCM calculations are shown in Table 7.3. Even in this implicit solvent model we observe antiferro- to ferro-magnetic crossover. It has been noticed that there is a difference between the computed crossover values ($\Delta J = J_{cis} - J_{trans}$) in PCM and ONIOM methods. The ONIOM being explicit in nature shows greater crossover (ΔJ) values. This is because of the fact that, instantaneous interaction of water molecule with that –OH group has an effect on the total energy values (for both singlet and triplet) of the trans

isomer. On the other hand, in PCM method all the diradicals of each and every pair are in same dielectric environment. It is evident from the PCM optimized spin density plots (Figure 7.3) that for the cis-diradicals the direct exchange interaction between the spin centers is predominant. However, for planer trans-isomers antiferromagnetic interaction is observed which is also in accordance with spin density alternation rules (Figure 7.3).[43]

Table 7.2. The ONIOM energies (in *au*) of all three different sets of diradicals and their corresponding $\langle S^2 \rangle$ values at UB3LYP/6-31G(d,p):UB3LYP/3-21G level of theory for inner core diradical and outer water layer respectively. All exchange coupling constants have been estimated in the unit of cm^{-1}.

Diradical		At (UB3LYP/6-31G(d,p):UB3LYP/3-21G) level		
		Energy(*au*)	$\langle S^2 \rangle$	$J(cm^{-1})$
1a	Triplet	−1592.37843	2.033	−6.6
	BS	−1592.37846	1.036	
1b	Triplet	−1592.38692	2.035	2.2
	BS	−1592.38691	1.036	
2a	Triplet	−1592.38116	2.037	−11
	BS	−1592.38121	1.040	
2b	Triplet	−1592.38587	2.034	4.4
	BS	−1592.38585	1.034	
3a	Triplet	−1517.58297	2.037	−8.8
	BS	−1517.58301	1.040	
3b	Triplet	−1517.58784	2.035	2.2
	BS	−1517.58783	1.035	

Table 7.3. The PCM optimization results for different trans and their respective cis forms of all studied diradicals in *blood plasma* (taking ε = 58) medium using UB3LYP/6-31G(d,p) level of theory. The $\langle S^2 \rangle$ values of each diradical are reported separately. The absolute energies are expressed in au, exchange coupling constants (J) in cm^{-1}.

Diradical		At UB3LYP/6-31G(d,p) level		
		Energy(*au*)	$\langle S^2 \rangle$	$J(cm^{-1})$
1a	Triplet	−1601.26522	2.037	−8.8
	BS	−1601.26526	1.040	
1b	Triplet	−1601.26938	2.039	2.2
	BS	−1601.26937	1.039	
2a	Triplet	−1601.26465	2.037	−6.6
	BS	−1601.26468	1.039	
2b	Triplet	−1601.26937	2.037	4.4
	BS	−1601.26935	1.037	
3a	Triplet	−1526.04072	2.037	−6.6
	BS	−1526.04075	1.040	
3b	Triplet	−1526.04523	2.038	2.2
	BS	−1526.04522	1.038	

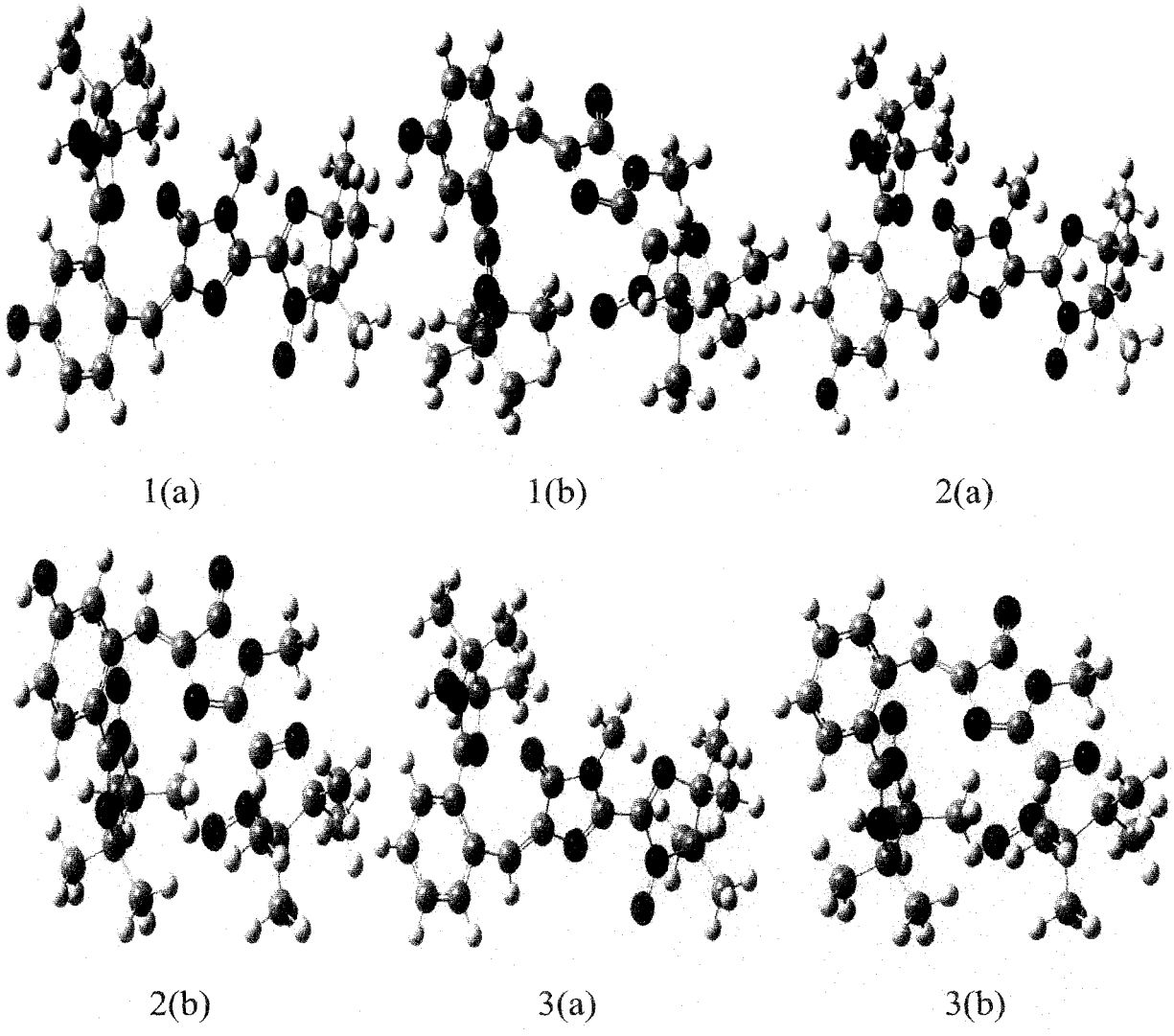

Figure 7.5. The PCM optimized geometries of three trans (1a, 2a, 3a) diradicals and their corresponding cis forms (1b, 2b, 3b) with different GFP variants (*p*-HBDI, *m*-HBDI and BFPF respectively) as coupler. The geometries are optimized using PCM method with ε = 58, at UB3LYP/6-31G(d,p) level of theory. The carbon atoms are represented in grey, nitrogen in blue, oxygen in red and hydrogen in white respectively.

7.3.1. Time Dependent Density Functional Study

As discussed earlier, the transition energies for the cis-trans conversion on irradiation of appropriate wave length of light can be estimated using TDDFT technique. The

experimentally found excitation peaks for different variants of neutral bare GFP used in the trans form of diradicals 1 and 3 are 399 nm and 355 nm respectively. By cautiously applying TDDFT technique we found a reasonably good match between the experimental findings[10(b),12(a)] and our calculated data. From the gas phase TDDFT results (Table 7.4), we conclude that with the application of 360-390 nm wave length of light the antiferromagnetic trans diradicals convert into their corresponding ferromagnetic cis forms. The transition brings out magnetic crossover along with a visual change from non-fluorescent dark to fluorescent green or blue form of GFP-diradicals. Similar types of calculations using water as solvent (Table 7.5) have been carried out for each pair of diradicals. A reasonable agreement between the experimental data[12(a)] and our calculated data for absorption wavelength of GFP at water medium at least for one example (1a) inspires about the authenticity of our calculation for rest of the molecules for which such experimental data are absent. For a visual effect, as all the trans forms of these diradicals are dark, upon irradiation of light of suitable wavelength the trans isomers change to corresponding bright fluorescent cis forms (green for *p*-HBDI and *m*-HBDI, blue for BFPF).[11,12] As a result, even without evaluating coupling constants, one can easily identify the magnetic status of the molecules, by visual inspection alone.

Table 7.4. The $\pi \rightarrow \pi^*$ transition energy values in gas phase, estimated wave length ${}^{a}\lambda_{exc}$ in trans diradicals at UB3LYP (TDDFT) level using 6-31G(d,p) basis set, ${}^{b}\lambda_{exc}$ is the experimental value for bare couple [ref. 12(a)].

Diradicals	E_{π} in *au*	E_{π^*} in *au*	Transition energy in *eV*	Estimated ${}^{a}\lambda_{exc}$ for diradicals in nm	Experimental ${}^{b}\lambda_{exc}$ for bare couplers in nm
1a	–0.20780	–0.08309	3.39353	364	392
2a	–0.21606	–0.08664	3.52170	351	–
3a	–0.21675	–0.08634	3.54864	349	355

Table 7.5. The estimated $\pi \rightarrow \pi^*$ transition energy values of all trans diradicals with wave length ${}^{a}\lambda_{exc}$ in water medium. Calculations are done at UB3LYP (TDDFT)/6-31G(d,p) level of theory, ${}^{b}\lambda_{exc}$ is the experimental value for bare coupler in water medium taken from ref. 12(a).

Diradicals	E_π in *au*	E_{π^*} in *au*	Transition energy in *eV*	Estimated ${}^{a}\lambda_{exc}$ for diradicals in nm	Experimental ${}^{b}\lambda_{exc}$ for bare couplers in nm
1a	–0.21875	–0.09473	3.37476	366	368
2a	–0.22717	–0.09679	3.54782	349	–
3a	–0.22843	–0.09715	3.57231	346	–

7.3.2. Applicability of the Designed Diradicals as Magnetic Resonance Imaging Contrast Agent (MRICA)

In this chapter, the ZFS parameter D and static ZFS magnitude (a_2) have been numerically estimated in gas phase, in water medium (with dielectric constant ε =80 and refractive index μ_{ri} = 1.33) and also in *blood plasma* medium (ε =58 and μ_{ri} = 1.1315),[44] (Table 7.6) for diradicals with S=1 states using ORCA program package[45] in DFT formalism. One point to be noted here is that, all the ferromagnetic diradicals possess the primary criterion to be a MRICA as discussed in the introduction section. Another point to be noted here is that, compared to nitroxide monoradical, nitroxide based di- or poly-radicals have the ability to increase the longitudinal relaxation rate ($1/T_{1e}$).[33(b)] A discussion about the D, a_2 and $1/T_{1e}$ is due here. The calculated D values and a_2 are reported in Table 7.6. It is apparent from the eq (7.9) that the static ZFS magnitude (a_2) is directly proportional to the longitudinal relaxation rate, (reciprocal of time taken for protons to realign with the external magnetic field, $1/T_{1e}$), which can be controlled in molecular level.[33(b)] Nonetheless, with the increase of $1/T_{1e}$ the observed MRI signal is enhanced.[46] From Table 7.6 it is evident that our computed $|D|$ values for cis diradicals are in the range of 1.62×10^{-2} to 1.69×10^{-2} cm^{-1} in

three different mediums. In an experimental work, Rajca and co-workers have synthesized nitroxide based high spin ($S = 1$) diradicals, which have been already established as standard MRICA of organic origin. In water ethanol mixture these synthesized diradicals have furnished the $|D|$ values in the range of 1.2×10^{-2} to 1.7×10^{-2} cm^{-1}.[33(a)] In another recent communication, we have noticed that, a stable diarylnitroxide triplet diradical is capable to be used as MRICA with $|D|$ and $|E|$ values 1.223×10^{-2} and 1.44×10^{-3} cm^{-1} correspondingly.[47] As a result, the calculated a_2 value for that diradical comes around 1.02×10^{-2} in the unit of cm^{-1}. In our designed GFP chromophore based diradicals, the calculated a_2 values are in the range of 1.33×10^{-2} to 1.39×10^{-2} cm^{-1} as depicted in Table 7.6. From these two experimental findings,[33(a),46] it is clear that, our designed diradicals are able to perform well as MRICA of organic origin, capable of producing clearer MRI image.[33(b),35] Moreover, each fragment of the diradicals i.e., the radical moieties[15,16] and the GFP fragments[11,13] both can cross the BBB. As a result, the constructed diradicals are also expected to cross the BBB and hence suitable as brain MRICAs.

Table 7.6. Spin-spin ZFS parameter $D^{(SS)}$ in cm^{-1}, static ZFS magnitude a_2 in cm^{-1} and rhombic ZFS parameter (E) values in cm^{-1} are given for all different ferromagnetic cis diradicals in three different mediums using UB3LYP/6-31G(d,p) basis set.

Diradicals	Medium	$D^{(SS)}$ in cm^{-1}	E in cm^{-1}	a_2 in cm^{-1}
	Gas	−0.01696	−0.00054	0.01387
1b	Water	−0.01682	−0.00053	0.01375
	Blood plasma	−0.01683	−0.00053	0.01376
	Gas	−0.01644	−0.00052	0.01344
2b	Water	−0.01628	−0.00051	0.01331
	Blood plasma	−0.01629	−0.00051	0.01332
	Gas	−0.01651	−0.00052	0.01350
3b	Water	−0.01636	−0.00051	0.01338
	Blood plasma	−0.01636	−0.00051	0.01338

7.4. Conclusions

In this chapter, we have designed and investigated three different pairs of photoswitchable antiferromagnetic trans and their corresponding ferromagnetic cis diradicals where GFP chromophore and its different fluorescent homologue are used as couplers with Imino Nitroxide (IN) as radical centers. The basis of choosing Imino Nitroxide (IN) as radical moiety lies on a report by Rajca et al., that the water soluble nitroxides can be used as very effective spin level, magnetic resonance imaging contrast agent, antioxidant etc.[47]

From our calculations we infer that all the designed diradicals are not only stable in different solvents but they also show antiferromagnetic to ferromagnetic crossover in different mediums like water (dielectric constant, $\varepsilon = 80$ and refractive index, $\mu_{ri} = 1.33$) and blood (dielectric constant, $\varepsilon = 58$ and $\mu_{ri} = 1.1315$),[44] when exposed to appropriate electromagnetic radiation. The calculations are done employing both ONIOM and PCM techniques. All the high spin geometries are optimized using UB3LYP/6-31G(d,p) method in ONIOM and PCM. The low spin states of these diradicals are described by ONIOM-BS and PCM-BS states. The photochemical properties of the diradicals in gas phase and in solvent phases have been investigated using TDDFT method.

We have investigated the possibility of using our designed diradicals as successful magnetic resonance imaging contrast agent. As of now, most of the widely used Gd-based MRICAs show adverse side effects due to Gd ions.[14] The designed diradicals, if synthesized, is expected to be free from such hazards. Rajca and co-workers[33(a)] have reported diradicals ($S = 1$) in water-ethanol mixture which can be used as MRICA. We found that our designed nitroxide based diradicals have static ZFS parameters D in the same range (1.2×10^{-2} to 1.7×10^{-2} cm^{-1}).[33(a)] The ZFS parameter is indicative of the efficiency of MRICA as already discussed. Moreover, the GFP chromophore is stable even at 65°C.[13] Thereby, these GFP based nano-magnetic moieties can be used in hyperthermia treatment where the therapeutic threshold is of 42°C.[1(a), 48] The GFP is also known to have good tagging ability,[13] thus magnetic separation of different GFP-tagged biological entity is possible with suitable use of these diradicals.

The concluding point to be discussed here has an ambitious note. The GFP encoded lentiviral particles paired with carbon coated Co-nanoparticle are used for therapeutic uses, particularly in the field of targeted gene delivery.[49] On the other hand, folate leveled magnetic nano-particles are used for their tagging ability in malignant cell without any side effects and toxicity.[50] As a matter of fact, one may combine these two ideas and converge to the point that if GFP based ferromagnetic diradicals tagged with folate moiety is injected without any biocompatible coating in a living organism, it can serve both these purposes. Nevertheless, this area is relatively young, rapidly developing, and multidisciplinary and can find a huge application in various fields if these diradicals are synthesized. The whole idea is represented in simple schematic manner by Scheme 7.3.

Scheme 7.3. The Schematic representation of bio-applicability of these six diradicals.

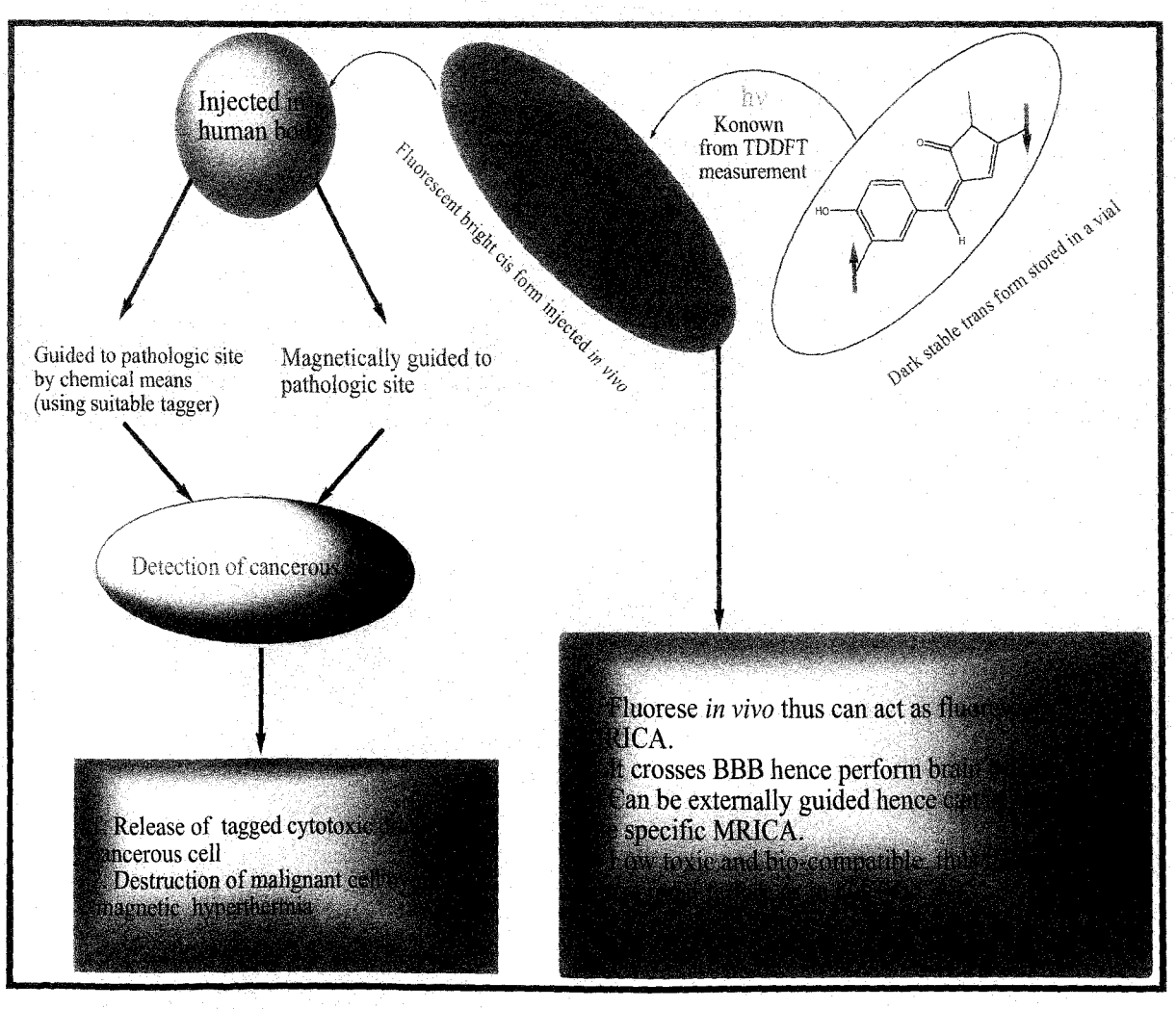

This work has been published in Physical Chemistry Chemical Physics (Ref. 51).

7.5. References and Notes

(1) (a) Pankhurst, Q. A.; Connolly, J.; Jones, S. K.; Dobson, J. *J. Phys. D: Appl. Phys.* **2003**, *36*, R167. (b) Tartaj, P.; Morales, M. P.; Veintemillas-Verdaguer, S.; González-Carreño, T.; Serna, C. J. *J. Phys. D: Appl. Phys.* **2003**, *36*, R182. (c) Pankhurst, Q. A.; Thanh, N. K. T.; Jones, S. K.; Dobson, J. *J. Phys. D: Appl. Phys.* **2009**, *42*, 224001.

(2) Salata, O. V. *J. Nanobiotechnol.* **2004**, *2*, 3.

(3) Jun, J.-W.; Seo, J.-W.; Cheon, J. *Acc. Chem. Res.* **2008**, *41*, 179.

(4) Palacio, F.; Miller, J. S. *Nature* **2000**, *408*, 421.

(5) (a) Shil, S.; Misra, A. *J. Phys. Chem. A* **2010**, *114*, 2022. (b) Bhattacharya, D.; Shil, S.; Misra, A. *J. Photochem. Photobiol. A: Chem.* **2011**, *217*, 402. (c) Saha, A.; Latif, I. A.; Datta, S. N. *Phys. Chem. A* **2011**, *115*, 1371.

(6) Thirion, C.; Wernsdorfer, W.; Mailly, D. *Nat. Mater.* **2003**, *2*, 524.

(7) Sato, O.; Iyoda, T.; Fujishima, A.; Hashimoto, K. *Science* **1996**, *272*, 704.

(8) (a) Tanifuji, N.; Matsuda, K.; Irie, M. *Polyhedron* **2005**, *24*, 2484. (b) Matsuda, K.; Irie, M. *Polyhedron* **200**^{5}, *24*, 2477. (c) Matsuda, K. *Bull. Chem. Soc. Jpn.* **2005**, *78*, 383. (d) Tanifuji, N.; Irie, M.; Matsuda, K. *J. Am. Chem. Soc.* **2005**, *127*, 13344. (e) Tanifuji, N.; Matsuda, K.; Irie, M. *Org. Lett.* **2005**, *7*, 3777.

(9) Ali, Md. E.; Datta, S. N. *J. Phys. Chem. A* **2006**, *110*, 10525.

(10) (a) Prasher, D. C.; Eckenrode, V. K.; Ward, W. W.; Pendergast, F. G.; Cormier, M. J. *Gene* **1992**, *111*, 229. (b) Tsien, R. Y. *Annu. Rev. Biochem.* **1998**, *67*, 509.

(11) (a) Tsien, R. Y. *FEBS Lett.* **2005**, *579*, 927. (b) Zimmer, M. *Glowing Genes: A Revolution in Biotechnology*; Prometheus Books: Amherst, NY, 2005. (c) Megley, C. M.; Dickson, L. A.; Maddalo, S. L.; Chandler, G. J.; Zimmer, M. *J. Phys. Chem. B* **2009**, *113*, 302.

(12) (a) Nifosí, R.; Amat, P.; Tozzini V. *J. Comput. Chem.* **2007**, *28*, 2366 and references therein. (b) Voliani, V.; Bizzarri, R.; Nifosí, R.; Abbruzzetti, S.; Grandi, E.; Viappiani, C.; Beltram, F. *J. Phys. Chem. B* **2008**, *118*, 10714.

(13) Zimmer, M. *Chem. Rev.* **2002**, *102*, 759, and references therein.

(14) Yerram, P.; Saab, G.; Karuparthi, P. R.; Hayden, M. R.; Khanna, R. *Clin. J. Am. Soc. Nephrol.* **2007**, *2*, 258.

(15) (a) Zhelev, Z.; Bakalova, R.; Aoki, I.; Matsumoto, K.; Gadjeva, V.; Anzai, K.; Kanno, I. *Mol. Pharmaceutics* **2009**, *6*, 504. (b) Zhelev, Z.; Bakalova, R.; Aoki, I.; Matsumoto, K.; Gadjeva, V.; Anzai, K.; Kanno, I. *Chem. Commun.* **2009**, 53.

(16) Konorev, E. A.; Tarpey, M. M.; Joseph, J.; Baker, J. E.; Kalyanaraman, B. *Free Rad. Bio. Med.* **1995**, *18*, 169.

(17) Lescope, C.; Luneau, D.; Rey, P.; Bussiere, G.; Reber, C. *Inorg. Chem.* **2002**, *41*, 5566.

(18) (a) Noodleman, L. *J. Chem. Phys.* **1981**, *74*, 5737. (b) Noodleman, L.; Baerends, E. J. *J. Am. Chem.* Soc. **1984**, *106*, 2316. (c) Noodleman, L.; Davidson, E. R. *Chem. Phys.* **1986**, *109*, 131. (d) Noodleman, L.; Peng, C. Y.; Case, D. A.; Mouesca, J.-M. *Coord. Chem. Rev.* **1995**, *144*, 199.

(19) (a) Yamaguchi, K.; Takahara, Y.; Fueno, T.; Nasu, K. *Jpn. J. Appl. Phys.* **1987**, *26*, L1362. (b) Yamaguchi, K.; Jensen, F.; Dorigo, A.; Houk, K. N. *Chem. Phys. Lett.* **1988**, *149*, 537. (c) Yamaguchi, K.; Takahara, Y.; Fueno, T.; Houk, K. N. *Theo. Chim. Acta.* **1988**, *73*, 337.

(20) (a) Martin, R. L.; Illas, F. *Phys. Rev. Lett.* **1997**, *79*, 1539. (b) Caballol, R.; Castell, O.; Illas, F.; Moreira, I. de P. R.; Malrieu, J. P. *J. Phys. Chem. A* **1997**, *101*, 7860. (c) Barone, V.; di Matteo, A.; Mele, F.; Moreira, I. de P. R.; Illas, F. *Chem. Phys. Lett.* **1999**, *302*, 240. (d) Illas, F.; Moreira, I. de P. R.; de Graaf, C.; Barone, V. *Theor. Chem. Acc.* **2000**, *104*, 265. (e) Illas, F.; Moreira, I. de P. R.; Bofill, J. M.; Filatov, M. *Phys. Rev. B* **2004**, *70*, 132414.

(21) (a) Polo, V.; Alberola, A.; Andres, J.; Anthony, J.; Pilkington, M. *Phys. Chem. Chem. Phys.* **2008**, *10*, 857. (b) Bhattacharya, D.; Misra, A. *J. Phys. Chem. A* **2009**, *113*, 5470. (c) Bhattacharya, D.; Shil, S.; Misra, A.; Klein, D. J. *Theor. Chem. Acc.* **2010**, *127*, 57. (d) Bhattacharya, D.; Shil, S.; Panda, A.; Misra, A. *J. Phys. Chem. A* **2010**, *114*, 11833.

(22) Ali, E. Md.; Oppeneer, P. M.; Datta, S. N. *J. Phys. Chem. B* **2009**, *113*, 5545.

(23) (a) Newton, M. D. *J. Chem. Phys.* **1973**, *58*, 5833. (b) Newton, M. D. *Annual Rev. Phys. Chem.* **1984**, *35*, 437.

(24) Mehta, N.; Datta, S. N. *J. Chem. Sci.* **2007**, *119*, 501.

(25) Parac, M.; Grimme, S. *J. Phys. Chem. A* **2002**, *106*, 6844.

(26) Stratmann, R. E.; Scuseria, G. E. *J. Chem. Phys.* **1998**, *109*, 8218.

(27) Slaughter, B. D.; Allen, M. W.; Lushington, G. H.; Johnson, C. K. *J. Phys. Chem. A* **2003**, *107*, 5670.

(28) Harbola, M. K. *Phys. Rev. B* **2002**, *65*, 052504.

(29) Casida, M. E.; Jamorski, C.; Casida, K. C.; Salahub, D. R. *J. Chem. Phys.* **1998**, *108*, 4439.

(30) Bauernschmitt, R.; Ahlrichs, R. *Chem. Phys. Lett.* **1996**, *256*, 454.

(31) Bauernschmitt, R.; Ahlrichs, R. *J. Chem. Phys.* **1996**, 104, 9047.

(32) Frisch, M. J.; Trucks, G. W.; Schlegel, H. B.; Scuseria, G. E.; Robb, M. A.; Cheeseman, J. R.; Scalmani, G.; Barone, V.; Mennucci, B.; Petersson, G. A.; Nakatsuji, H.; Caricato, M.; Li, X.; Hratchian, H. P.; Izmaylov, A. F.; Bloino, J.; Zheng, G.; Sonnenberg, J. L.; Hada, M.; Ehara, M.; Toyota, K.; Fukuda, R.; Hasegawa, J.; Ishida, M.; Nakajima, T.; Honda, Y.; Kitao, O.; Nakai, H.; Vreven, T.; Montgomery, J. A.; Jr., Peralta, J. E.; Ogliaro, F.; Bearpark, M.; Heyd, J. J.; Brothers, E.; Kudin, K. N.; Staroverov, V. N.; Keith, T.; Kobayashi, R.; Normand, J.; Raghavachari, K.; Rendell, A.; Burant, J. C.; Iyengar, S. S.; Tomasi, J.; Cossi, M.; Rega, N.; Millam, J. M.; Klene, M.; Knox, J. E.; Cross, J. B.; Bakken, V.; Adamo, C.; Jaramillo, J.; Gomperts, R.; Stratmann, R. E.; Yazyev, O.; Austin, A. J.; Cammi, R.; Pomelli, C.; Ochterski, J. W.; Martin, R. L.; Morokuma, K.; Zakrzewski, V. G.; Voth, G. A.; Salvador, P.; Dannenberg, J. J.; Dapprich, S.; Daniels, A. D.; Farkas, O.; Foresman, J. B.; Ortiz, J. V.; Cioslowski, J.; Fox, D. J. Gaussian 09 W, revision B.01; Gaussian, Inc.: Wallingford CT, 2010.

(33) (a) Spagnol, G.; Shiraishi, K.; Rajca, S.; Rajca, A. *Chem. Commun.* **2005**, 5047. (b) Olankitwanit, A.; Kathirvelu, V.; Rajca, S.; Eaton, G. R.; Eaton, S. S.; Rajca, A. *Chem. Commun.* **2011**, *47*, 6443.

(34) Duboc, C.; Ganyushin, D.; Sivalingam, K.; Collomb, M.; Neese, F. *J. Phys. Chem. A* **2010**, *114*, 10750.

(35) Tucker, B. J. *Dissertation in Chemistry in the Graduate College of the University of Illinois at Urbana-Champaign*, 2010.

(36) Zein, S.; Duboc, C.; Lubitz, W.; Neese, F. *Inorg. Chem.* **2008**, *47*, 134.

(37) Loboda, O.; Minaev, B.; Vahtras, O.; Schimmelpfennig, B.; Ågren, H.; Ruud, K.; Jonsson, D. *Chem. Phys.* **2003**, *286*, 127.

(38) Harriman, J. E. *Theoretical Foundations of Electron Spin Resonance*, Academic Press, New York, 1987.

(39) McWeeny, R.; Mizuno, Y. *Proc. R. Soc.*, London, **1961**, *A259*, 554.

(40) Boča, R. *Theoretical Foundations on Molecular Magnetism*, Elsevier, 1999.

(41) Benmelouka, M.; Borel, A.; Moriggi, L.; Helm, L.; Merbach, A. E. *J. Phys. Chem. B* **2007**, *111*, 832.

(42) Belorizkya, E.; Fries, P. H. *Phys. Chem. Chem. Phys.* **2004**, *6*, 2341.

(43) (a) Klein, D. J.; Nelin, C. J.; Alexander, S.; Matsen, F. A. *J. Chem. Phys.* **1982**, *77*, 3101. (b) Trindle, C.; Datta, S. N. *Int. J. Quantum Chem.* **1996**, *57*, 781. (c) Trindle, C.; Datta, S. N.; Mallik, B. *J. Am. Chem. Soc.* **1997**, *119*, 12947.

(44) Jin, Y. L.; Chen, J . Y.; Xu, L.; Wang, P. N. *Phys. Med. Biol.* **2006**, *51*, N371.

(45) Neese, F. *ORCA – an ab-initio density functional and semiempirical program package*, Version 2.8-20; Max-Planck institute for bioinorganic chemistry, Mulheim an der Ruhr, Germany, 2010.

(46) (a) Bottrill, M.; Kwok, L.; Long, N. J. *Chem. Soc. Rev.* **2006**, *35*, 557. (b) Hanaoka, K.; Kikuchi, K.; Terai, T.; Komatsu, T.; Nagano, T. *Chem. Eur. J.* **2008**, *14*, 987.

(47) Rajca, A.; Shiraishi, K.; Rajca, S. *Chem. Commun.* **2009**, 4372.

(48) (a) Kar, R.; Misra, A. *J. Magn. Magn. Mater.* **2010**, *322*, 671. (b) Kar, R.; Misra, A. *Nanosci. Nanotechnol. Lett.* **2010**, *2*, 253.

(49) Weber, W.; Lienhart, C.; Baba, M. D.; Grass, R.N.; Kohler, T.; Muller, R.; Stark, W. J.; Fussenegger, M. *J. Biotechnol.* **2009**, *141*, 118.

(50) Mohapatra, S.; Mallick, S. K.; Maiti, T. K.; Ghosh, S. K.; Pramanik, P. *Nanotechnology* **2007**, *18*, 385102.

(51) Bhattacharya, D.; Panda, A.; Shil, S.; Goswami, T.; Misra, A. *Phys. Chem. Chem. Phys.* **2012**, *14*, 6509.